

Anbarasu Prema¹, Raghunathan Muthuselvi^{2*},
Ramaswami Vashantha³

¹Government Arts College for Women, Nilakkottai, Tamilnadu, India, ²Sri Meenakshi Government Arts College for Women (A), Madurai, Tamilnadu, India, ³Anna Adarsh College for Women, Chennai, India

Scientific paper

ISSN 0351-9465, E-ISSN 2466-2585

<https://doi.org/10.62638/ZasMat1179>



Zastita Materijala 65 (3)
389 - 398 (2024)

Synthesis and characterization of copper nanoparticle of *Solanum Virginianum* and *Coccinia Grandis* extract: A comparative study of thermal behavior

ABSTRACT

A Biogenic, green synthesis method is described for the novel copper nanoparticles from the leaf extract of *Solanum Virginianum* and *Coccinia Grandis*. Fourier-Transform Infrared spectroscopy and Thermal gravimetric analysis were used to examine the resultant nanoparticles. Compositional analysis and the study of processes like vaporization and decomposition were both accomplished by thermogravimetric analysis. The volatile compounds that the sample released was analyzed using TGA in conjunction with Fourier transform infrared spectroscopy (FTIR). From the FTIR data obtained it showed that the CG-CuNPs and SV-CuNPs both included functional molecular structure. Additionally, the TGA results showed that SV-CuNPs and CG-CuNPs exhibit effective thermal stability behavior, while the plant extracts from *Coccinia grandis* and *Solanum virginianum* play a major role in the creation of nanoparticles and also enhance their thermal stabilities.

Keywords: *Coccinia grandis*, *Solanum virginianum*, green synthesis, Copper nanoparticles, thermal analysis

1. INTRODUCTION

Nanotechnology finds application in different areas like health care, cosmetics, drug-gene delivery, energy science, optoelectronics, photocatalyst property etc., [1]. Nanoparticles are of great interest due to their extremely small size and large surface area to volume ratio, which lead to both chemical and physical differences in their properties (e.g. mechanical properties, biological and sterical properties, catalytic activity, thermal and electrical conductivity, optical absorption and melting point) compared to bulk of the same chemical composition. Therefore, design and production of materials with novel applications can be achieved by controlling shape and size at nanometer scale. Nanoparticles exhibit size and shape-dependent properties which are of interest for applications ranging from bio sensing and catalysts

to optics, antimicrobial activity, computer transistors, electrometers, chemical sensors, and wireless electronic logic and memory schemes. These particles also have many applications in different fields such as medical imaging, nanocomposites, filters, drug delivery, and hyperthermia of tumors fields such as medical imaging, nanocomposites, filters, drug delivery, and hyperthermia of tumors [2].

Nowadays metal nanoparticles are gaining huge attraction in various fields due to their extremely small size. Further research works are being carried by scientists all over the world about further applications of these nanoparticles. Many researchers have reported the synthesis of nanoparticles using toxic chemicals as a reducing and stabilizing agent. As a result, the environment becomes polluted and furthermore nurturing apprehensions to living beings and aquatic life. Thus, it is very much essential to develop environmentally friendly process. The chemical synthesis of nanoparticle resulted in toxic and less effective nanoparticles [1], Chemical reduction method gives good results for the synthesis of nanoparticles, but use of hazardous, reducing,

*Corresponding author: Raghunathan Muthuselvi

E-mail: muthuselvi@mashankar@gmail.com

Paper received: 29. 10. 2023.

Paper corrected: 12. 04. 2024.

Paper accepted: 12. 05. 2024.

Paper is available on the website: www.idk.org.rs/journal

costly and protecting agent makes the process toxic. To avoid the use of toxic reagent for the synthesis of nanoparticles [3], Green synthesis of nanoparticle is eco-friendly and less toxic. The green synthesis of nanoparticle depends on the selection of substances which are nontoxic, solvents and reducing agent for stability of silver nanoparticles. The experiment is designed to validate the applications of folklore medicine to control the prevalence of diseases. But, the synthesis from plant extracts became the best method due to the efficacy in the reduction of metal ions by the principle biomolecules present in plant extracts and usage of no chemicals that are harmful to the living organisms and environment. Earlier reports suggest that the *Coccinia grandis* has been widely studied for its pharmacological activities and regarded as Universal Panacea in Ayurvedic. The plant parts of *Coccinia grandis* such as leaves, fruits, and roots possess antioxidant, antimalarial, anthelmintic, antipyretic, antiulcer, anticancer and antibacterial activities, etc. [23, 24] Hence, the present study aimed to synthesize gold nanoparticles and studying their characterization and catalytic activity [4].

The *Coccinia grandis* commonly called as Ivy guard, is used as vegetable and grown in South Asia. It is a creeping plant. All the parts of the plant are edible and have got various medicinal uses such as anti-bruises and anti-itching from insect bites, treatment against cataract, skin diseases such as leprosy, fever, jaundice, mast cell-stabilizing, antianaphylactic and antihistaminic potential, urinary tract infections, respiratory tract infections, ulcerations etc., Similarly, it is used as an antioxidative, anti-inflammatory and antimicrobial agent and very limited information is available on its anti-diabetic effect so the present study aimed to analyse the antidiabetic activities in vitro. In addition to this its antimicrobial activities were also studied using the two different extracts such as ethanolic and isopropyl alcohol extracts of *Coccinia grandis* [5].

Coccinia grandis is a type of plant belonging to the Cucurbitaceae (commonly known as ivy gourd). This plant has also medicinal value in curing eczema, tongue sores and cerebral oxidative stress. The stem and root of ivy gourd are used in skin disease, asthma, bronchitis, joint pains, and many others. *Coccinia grandis* contains important raw materials, such as alkaloids, glycoside and saponin, bamyrene, lupeol, cucubbitacin, cephalandrol, cephalandrine and flavonoids for drug production [3,6]. In recent, green synthesis of Cu nanoparticles was achieved by using microorganisms, plant extract, bio-waste

and medicinal leaf extract. *Coccinia grandis* (local name Ivy gourd) is a traditional medicinal plant of India has a source of bio-reduction and stabilizers [7].

Solanum virginianum is a very prickly perennial herb with woody base plant from the family Solanaceae which is common throughout India, Sri Lanka, Burma, Malaysia and Nepal. The plant is used in rheumatism, asthma, also as diuretic, anthelmintic and anti-inflammatory substance. The aerial parts and the roots are used in herbal preparations. *S. virginianum* is endowed with various chemical components such as alkaloids, flavonoids, phytosterols, mucilage and fixed oil etc., which possibly contribute to its vast uses in folklore medicine [8]. *Solanum virginianum* (Solanaceae), commonly called as 'Kantakari', is an itchy perennial herb. This herb is also called as 'Indian night shade' or 'yellow berried night shade' plant. Different parts of this plant are a rich source of varied phytochemicals viz. phenols, saponins, terpenoids, alkaloids, flavonoids, glycosides, and amino acids. In Ayurvedic system of medicine, this whole plant is used as antimicrobial, antitumor, antipyretic, anti-inflammatory, anti-allergy, anti-fertility, hypoglycaemic, antioxidant, and anti-histamine agents. In addition, the plant is used for treating asthma, skin infection, headache, hair fall, and cough too. Fruits of *Solanum* spp. are known to exhibit several biological traits, including anthelmintic, wound healing, antipyretic, laxative, anti-asthmatic, antibacterial, antioxidant, larvicidal, anti-inflammatory, anti-diabetic, hepatoprotective, anti-urolithiatic, anti-fertility and aphrodisiac activities. In fact, fruits of this *Solanum* spp. contain plethora of effective bioactive phytochemicals such as solanosine, solasodine, carpesterol, campesterol, daucosterol, caffeic acid, coumarins, triterpenoids, solanocarpine, solamorgine, solanocarpidine, lupeol, and diosgenine which are considered potent therapeutic agents [9].

Thus, this article reports a green method for the synthesis of copper nanoparticles (CuNPs) and using novel *Coccinia grandis* and *Solanum virginianum* plant extract [3]. To the best of our knowledge, the use of *Coccinia grandis* and *Solanum virginianum* plant extract for greener synthesis of Cu nanoparticles has not been reported. Hence the present study was carried out to synthesize and characterize the copper nanoparticles using *Coccinia grandis* and *Solanum virginianum* plant extract. Further, characterized using thermogravimetric analysis of both copper loaded *Coccinia grandis* and *Solanum virginianum* plant extract. Finally, in this work, *Coccinia grandis* and *Solanum virginianum* plant extract are mainly responsible for

the formation of nanoparticles and also having the enhancement of their thermal stabilities [7].

2. MATERIAL AND METHODS

2.1. Collection and processing of plant material

From the Periyakulam District of Tamilnadu State of India, whole plant samples of *Solanum Virginianum* (SV) and *Coccinia Grandis* (CG) (Fig.1) were gathered. The collected leaves were transported to the study facility and stored in a glass bottle with a tight closure. After that, it was cleaned twice with distilled water to get rid of any remaining dust, and it was left to dry for two weeks at room temperature under dark conditions. The leaves were then roughly ground in an electric blender and kept apart in a sealed container for later use



Figure 1. *Solanum Virginianum* (SV) and *Coccinia Grandis* (CG) leaves

2.2. Preparation of Leaf Extract

An Erlenmeyer flask containing 100 ml of distilled water was filled with one gram of the powdered leaves that had been gathered. It is heated to between 60 and 80°C while being agitated for roughly 20 minutes using a magnetic stirrer and hotplate. After that, the stirrer is withdrawn, and it cools. The solution was filtered using Whatman No. 40 filter paper once it had cooled. The filter, which has a brown colour, is called leaves extract.

2.3. Preparation of 1/20 CuSO₄ solution

By precisely weighing 0.0499g of CuSO₄.5H₂O, a 1mM solution of copper was created and added to 200 mL in a conventional measuring flask.

2.4. Synthesis of Copper nanoparticles

In The reaction mixture, 20 mL of leaves extract was added to 20 mL of 1mM CuSO₄ solution, the blank solution was prepared in a similar manner by adding 20 mL of distilled water to 20 mL of Leaves extract. Using a magnetic stirrer, the mixture was heated to 80°C while being continuously stirred for one hour. The change of colour to brown precipitate indicated the formation of copper nanoparticles (CuNPs). After few hours, the nanoparticles colour changed from brown to black and settled at the bottom of the reaction flask (Fig.2) that was filtered with whatman 40 filter paper, dried and transferred to a clean and dry container for further studies.

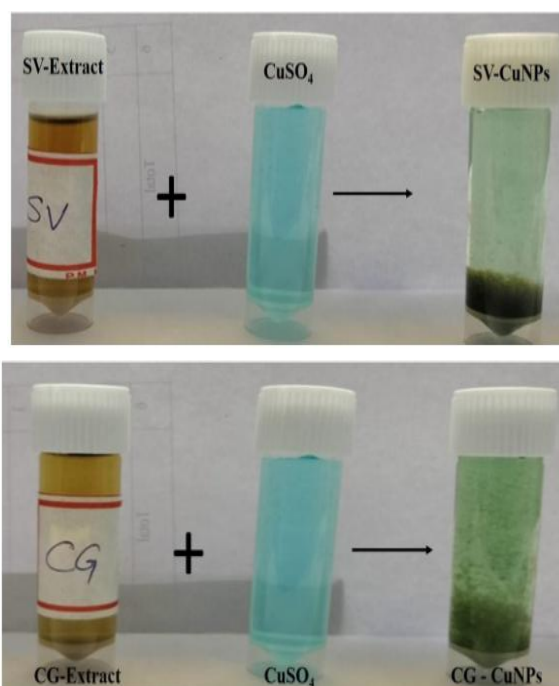


Figure 2. Copper nanoparticles (CuNPs) of SV and CG leaves

2.5. Kinetic Parameters calculated from modified form of Coats and Redfern model

The SV-CuNPs and CG-CuNPs prepared plant extract powder were subjected to thermogravimetric analysis under nitrogen gas 10 °C per minutes. SV-CuNPs and CG-CuNPs were tested at different heating rates of 10 – 50 °C per minutes. Considering all phase transformations as 1st order reactions, activation energy and other thermodynamic parameters were determined using 1st order reaction rate equation as given in equation [10]

$$dx/dt = K(1-x) \quad (1)$$

where,

$$x = wi-wt/Wi-wf \quad (2)$$

and w_i is the initial weight, w_t is weight of sample at particular time t and w_f is final weight. equation 11 can be rewritten as

$$\ln(1 - x) = -kt \quad (3)$$

Kinetics parameters were determined using modified form of Coats and Redfern model as described in equation [10]

$$\ln[-\ln(1 - x)] = \ln \frac{ART^L}{\beta E\alpha} - \frac{E\alpha}{RT} \quad (4)$$

where, A is pre-exponential factor, β is heating rate ($10^\circ - 50^\circ/\text{min}$), R is general gas constant ($8.3143 \text{ J mol}^{-1} \text{ K}^{-1}$), E_a is activation energy and T is temperature (K). Plotting graphs between $\ln[-\ln(1 - x)]$ vs $10000/T$ for each phase. The resultant graph gave the value of activation energy and further parameters were determined using basic thermodynamic equations.

3. RESULT AND DISCUSSION

3.1. FT-IR analysis of SV-CuNPs and CG-NPs

The FT-IR spectrum of SV and CG CuNPs plant extract show (Fig. 3 and 4) the absorption band position at 3329 and 3160 cm^{-1} denoting the alcoholic (O-H) or phenolic (O-H) stretching vibration presence in the plant extract. A small absorption band solder are observed at 2854 cm^{-1} which suggested the C-H stretching frequency present in the plant extract. The band located at 1618 cm^{-1} and 1621 cm^{-1} reveals C=O stretching vibration of aliphatic and aromatic amides and possible binding of CuNPs with the proteins present in the extract. The N-H wagging or out of plane O-H bending vibration are positioned at 652 cm^{-1} , which has been confirmed by the CG plant extract [7].

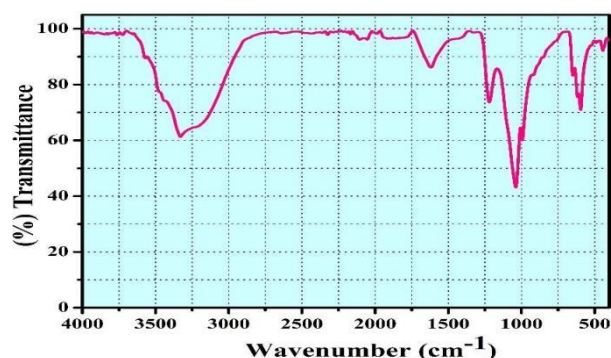


Figure 3. FT-IR spectrum of SV-CuNPs

The absorption band position at 1039 cm^{-1} confirms the presence of stretching vibration of primary amine, C≡N in the plant extract of SV [11].

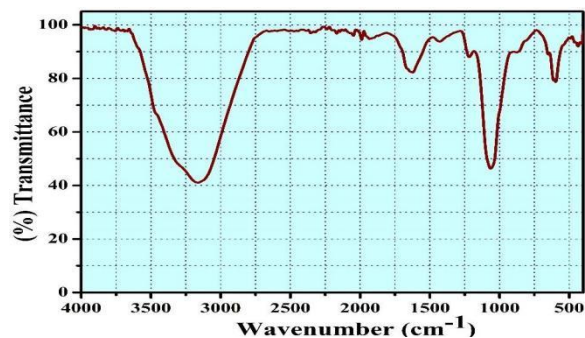


Figure 4. FT-IR spectrum of CG-CuNPs

3.2. Thermogravimetric analysis of SV-CuNPs

The different heating rate of thermogram prepared for SV-CuNPs has been recorded (Fig.5) and the weight loss are tabulated in Table 1. The three stage degradation are observed from the thermogram pattern. The first stage of degradation observed at temperature range between $30 - 100^\circ \text{C}$ and the weight loss obtained is of 10.06, 9.33, 7.83, 7.75 and 6.36% due to loss of moisture present in the prepared SV-CuNPs at the heating rate 10, 20, 30, 40 and 50°C respectively. The second stage weight loss predicted from $100 - 450^\circ \text{C}$ is due to loss of alkaloid present in the SV-CuNPs and the weight loss observed is of 46.10, 49.13, 48.38, 46.19 and 42.44% at heating rate 10, 20, 30, 40 and 50°C respectively.

Table 1. The weight loss of SV-CuNPs at different heating rate ($10 - 50^\circ \text{C}$)

S. No.	Heating Rate ($^\circ\text{C}/\text{min}$)	Temperature ($^\circ\text{C}$)			Total weight loss (%)	Residue (%)
		Weight loss (%)				
		30 - 100	100 - 450	450 - 800	30 - 800 ($^\circ\text{C}$)	
1	10	10.06	46.10	11.87	68.03	31.97
2	20	9.33	49.13	13.22	71.68	28.32
3	30	7.83	48.38	11.71	67.92	32.08
4	40	7.75	46.19	10.18	64.12	35.88
5	50	6.36	42.44	12.18	60.98	39.02

The third stage weight loss observed of 68.03, 71.68, 67.92, 64.12 and 60.98% at heating rate 10, 20, 30, 40 and 50°C respectively has been observed at temperature range between $450 - 600^\circ \text{C}$ due to loss of CuNPs present in the SV-CuNPs. This has been confirmed from the alkaloid present in the prepared SV-CuNPs [12]. The weight loss differ for different heating rate due to fast decomposition of the SV-CuNPs and the total weight loss observed from $30 - 600^\circ \text{C}$ is 68.03, 71.68, 67.92, 64.12 and 60.98% at heating rate of 10, 20, 30, 40 and 50°C . The maximum residue observed is of 39.02% at heating rate $50^\circ \text{C}/\text{min}$.

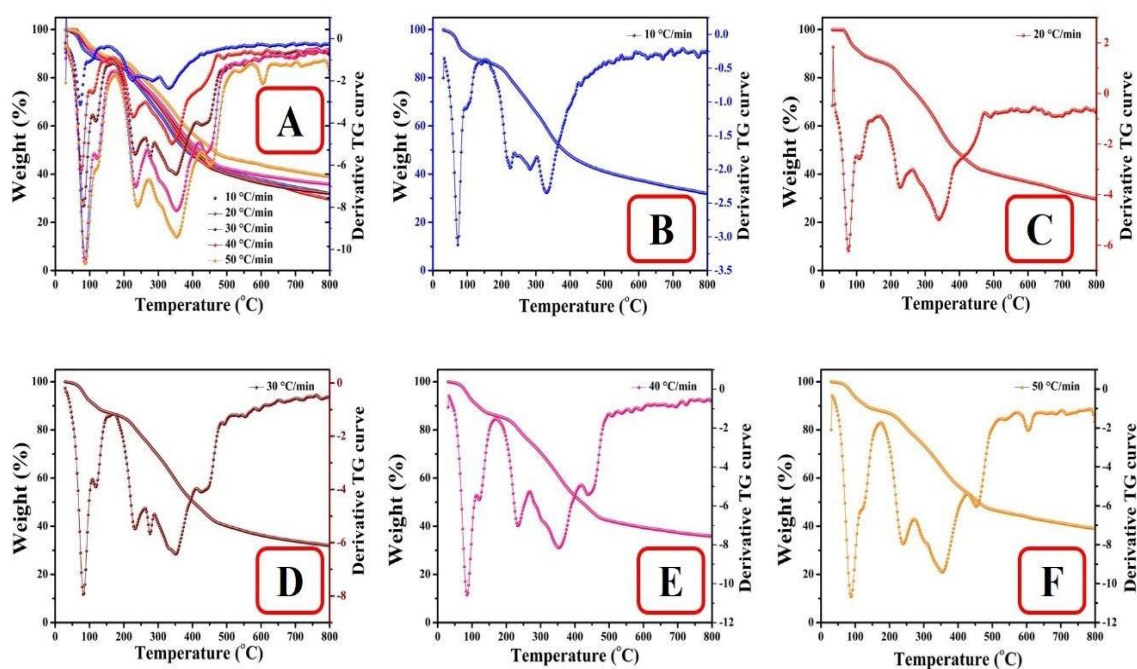


Figure 5. Thermogram of SV CuNPs of different heat rate A) Overall heating rate (10 – 50 °C) B) SV-CuNPs 10 °C/min, C) SV-Cu NPs 20 °C/min, D) SV-Cu NPs 30 °C/min, E) SV-Cu NPs 40 °C/min, F) SV-Cu-NPs 50 °C/min

The plot of $\ln[-\ln(1 - x)]$ vs $1000/T$ at different heating rate of SV-CuNPs are graphically recorded (Fig. 6). Activation energy (E_a), Free energy (ΔG), Enthalpy (ΔH) and Entropy (ΔS) of SV-CuNPs are calibrated via thermal analysis at different heating rate at 100 °C (Phase I), 250°C (Phase II), 600°C

(Phase III) (Fig.7). Their corresponding values are tabulated in Table 2. The different heating rate of SV-CuNPs obtained from Gibbs free energy are shown in positive values in the range of 98.0920 to 238.5327 kJ mol^{-1} which is a thermally non-spontaneous process.

Table 2. Thermodynamic parameters of SV-CuNPs at different heating rate at temperature (100, 250 and 600°C)

S. No	Heating rate(°C/min)	phase	Temp.(°C)	E_a (kJ mol^{-1})	ΔS (kJ mol^{-1})	ΔH (kJ mol^{-1})	ΔG (kJ mol^{-1})
1	10	1	100	67.3290	-0.0821	64.2278	94.8633
		2	250	7.1086	-0.2806	2.7603	149.4962
		3	600	17.9489	-0.2610	10.6905	238.5327
2	20	1	100	63.3658	-0.1039	60.2645	99.0108
		2	250	7.4205	-0.2802	3.0721	149.6095
		3	600	18.9250	-0.2598	11.6666	238.4543
3	30	1	100	62.2849	-0.1047	59.1837	98.2535
		2	250	8.8234	-0.2750	4.4750	148.2745
		3	600	20.9146	-0.2551	13.6562	236.4001
4	40	1	100	64.3884	-0.0987	61.2872	98.0920
		2	250	10.0470	-0.2699	5.6986	146.8811
		3	600	20.8689	-0.2546	13.6105	235.8893
5	50	1	100	66.5967	-0.0936	63.4955	98.4098
		2	250	9.5598	-0.2722	5.2114	147.5908
		3	600	20.5396	-0.2559	13.2813	236.6666

The lowest value of ΔG 98.0920 kJ mol^{-1} is observed at heating rate of 40 $^{\circ}\text{C/min}$ in Phase I. The negative values of Entropy (ΔS) is observed in the range of -0.0821 to -0.2806 kJ mol^{-1} at heating rate of 10 $^{\circ}\text{C/min}$ in Phase I and Phase II correspondingly. The positive values of Enthalpy (ΔH) are observed in the range of 2.7603 to 64.2278 kJ mol^{-1} .

The lowest and highest values of ΔH are observed in the heating rate of 10 $^{\circ}$ /min in Phase I and II respectively. Maximum and minimum E_a values are observed at 67.3290 and 7.1086 kJ mol^{-1} at heating rate 10 $^{\circ}\text{C/min}$ in Phase I and II respectively.

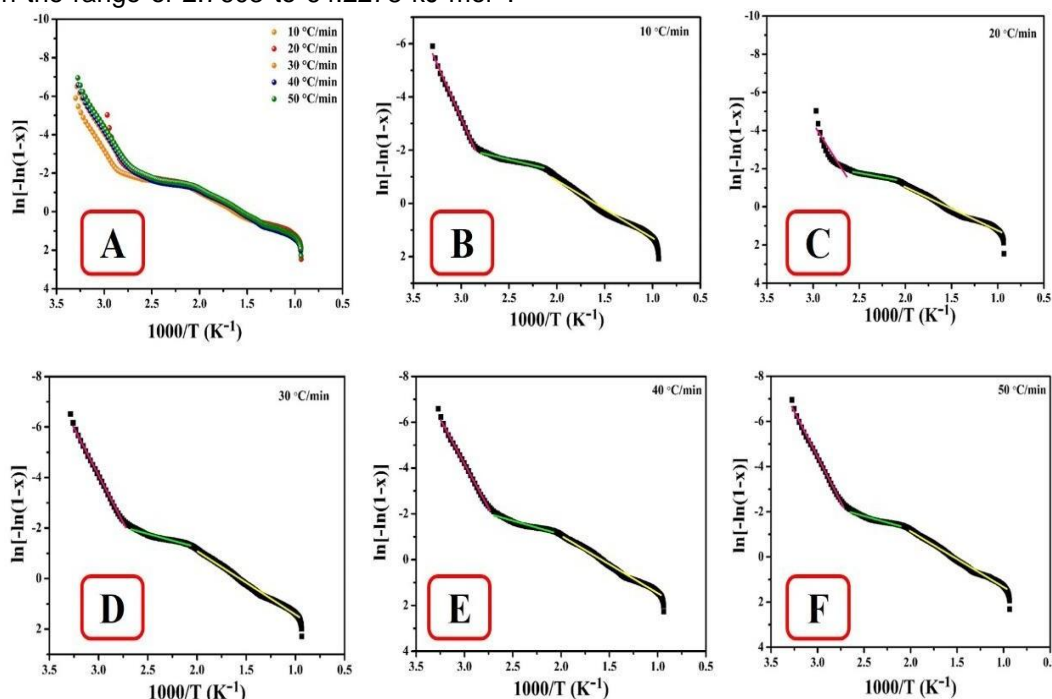


Figure 6. Plot of $\ln[-\ln(1-x)]$ vs $1000/T$ at different heating rate of SV-CuNPs A) Overall heating rate (10 – 50 $^{\circ}\text{C}$) B) SV-CuNPs 10 $^{\circ}\text{C/min}$, C) SV-Cu NPs 20 $^{\circ}\text{C/min}$, SV-Cu NPs 30 $^{\circ}\text{C/min}$, E) SV-CuNPs 40 $^{\circ}\text{C/min}$, F) SV-Cu NPs 50 $^{\circ}\text{C/min}$

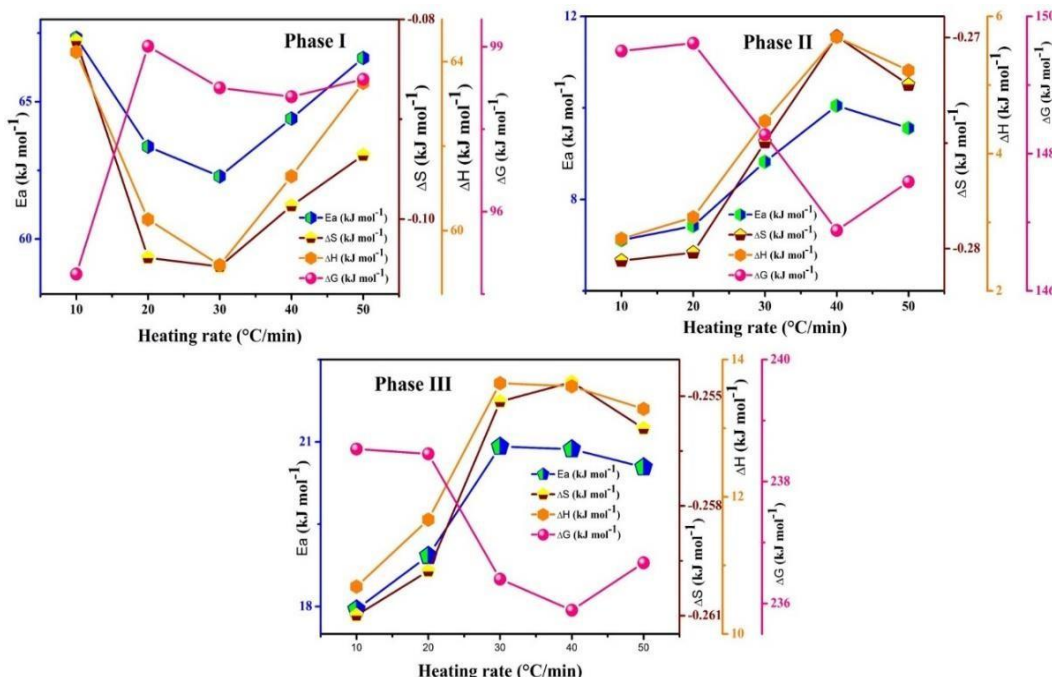


Figure 7. Thermal parameter of different heating rate at 100 $^{\circ}\text{C}$ (Stage I), 250 $^{\circ}\text{C}$ (Phase II) and 600 $^{\circ}\text{C}$ (Phase III)

3.3. Thermogravimetric analysis of CG-CuNPs

The different heating rate thermogram of CG-CuNPs (Fig. 8) has been recorded and the weight loss has been tabulated in Table 3. The three stage degradation were observed from thermogravimetric analysis. The first stage of degradation observed at temperature range between 30 – 100 °C and the weight loss obtained of 16.25, 12.70, 11.87, 12.18 and 11.32% is due to loss of moisture present in the prepared CG-CuNPs at the heating rate 10, 20, 30, 40 and 50 °C in that order. The second stage weight loss predict from 100–450°C, due to loss of hemicellulose present in the CG-CuNPs and the weight loss is observed of 26.38, 42.35, 44.83, 43.74 and 42.30% at heating rate 10, 20, 30, 40

and 50 °C correspondingly. The third stage weight loss observed of 16.04, 11.79, 11.83, 14.03 and 13.02% at heating rate 10, 20, 30, 40 and 50 °C respectively, has been observed at temperature range between 450 – 600 °C due to loss of CuNPs present in the CG-CuNPs. This has been confirmed the hemicellulose and CuNPs present in the prepared CG-CuNPs [13]. The weight loss differs from different heating rate due fast decomposition of the CG-CuNPs and the total weight loss observed from 30 – 600 °C is of 58.67, 66.84, 68.53, 69.95 and 66.64% at heating rate 10, 20, 30, 40 and 50°C correspondingly. The maximum residue is observed of 41.33% is at heating rate 10 °C/min.

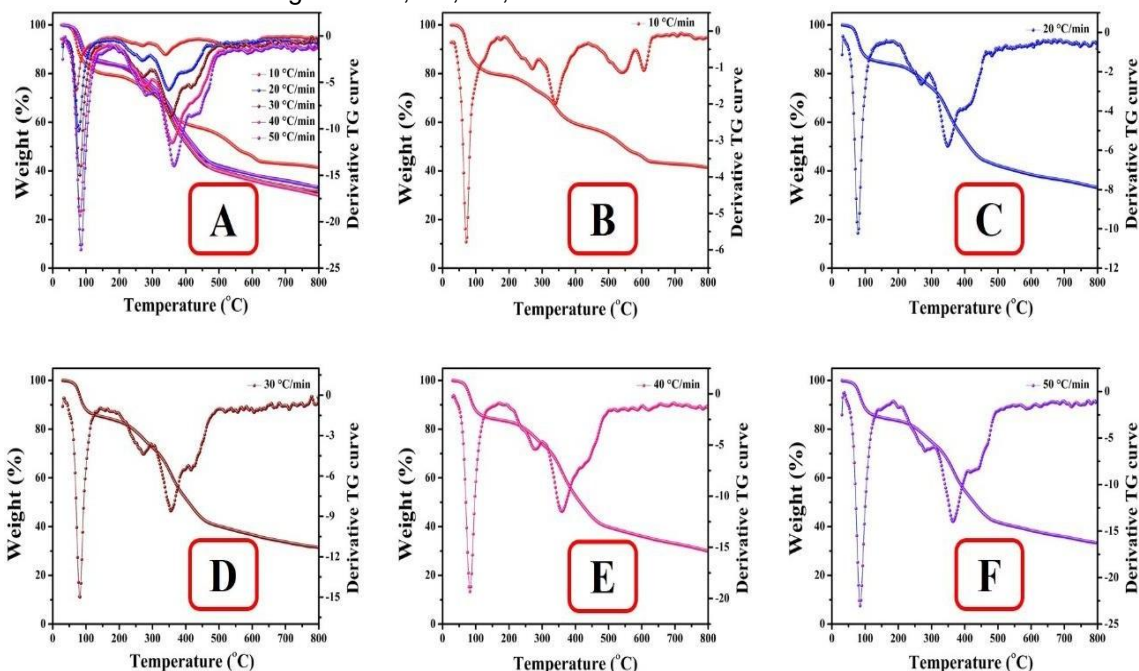


Figure 8. Thermogram of CG-CuNPs of different heat rate A) Overall heating rate (10– 50°C) B) CG-NPs 10°C/min, C) CG-NPs 20°C/min, D) CG-NPs 30°C/min, CG-NPs 40°C/min, F) CG-NPs 50°C/min

Table 3. The weight loss of CG-CuNPs at different heating rate (10 – 50 °C)

S. No.	Heating Rate (°C/min)	Temperature (°C)			Total weightloss (%)	Residue(%)
		Weight loss (%)				
		30 - 100	100 - 450	450 - 800	30 - 800 (°C)	
1	10	16.25	26.38	16.04	58.67	41.33
2	20	12.70	42.35	11.79	66.84	33.16
3	30	11.87	44.83	11.83	68.53	31.47
4	40	12.18	43.74	14.03	69.95	30.05
5	50	11.32	42.30	13.02	66.64	33.36

The plot of $\ln[-\ln(1-x)]$ vs $1000/T$ at different heating rate of CG-CuNPs (Fig. 9) has been recorded and depicted. Activation energy (E_a), Free energy (ΔG), Enthalpy (ΔH) and Entropy (ΔS) of CG-CuNPs are calibrated via thermal analysis at different heating rate of 100 °C (Phase I), 250°C (Phase II), 600°C (Phase III) (Fig.10), the resultant

values are tabulated Table 4. The different heating rate of CG-CuNPs obtained Gibbs free energy are shown in positive values in the range of 92.3674 to 237.5184 kJ mol^{-1} which has been thermally non spontaneous process. The lowest value of ΔG 92.3674 kJ mol^{-1} is observed at heating rate 10°C/min in Phase I. The negative change in

Entropy (ΔS) values is observed in the range of -0.0202 to -0.2958 kJ mol^{-1} , which has been observed at heating rate 30 $^{\circ}\text{C}/\text{min}$ in Phase I and Phase III correspondingly. The positive Enthalpy (ΔH) values are observed in the range of 0.0607 to 86.8146 kJ mol^{-1} . The lowest and highest values of

ΔH are observed in the heating rate 10 $^{\circ}$ and 30/min from Phase II and I respectively. Maximum and minimum E_a value is observed of 89.9158 and 4.4091 kJ mol^{-1} at heating rate 30 and 10 $^{\circ}\text{C}/\text{min}$ form Phase I and II respectively.

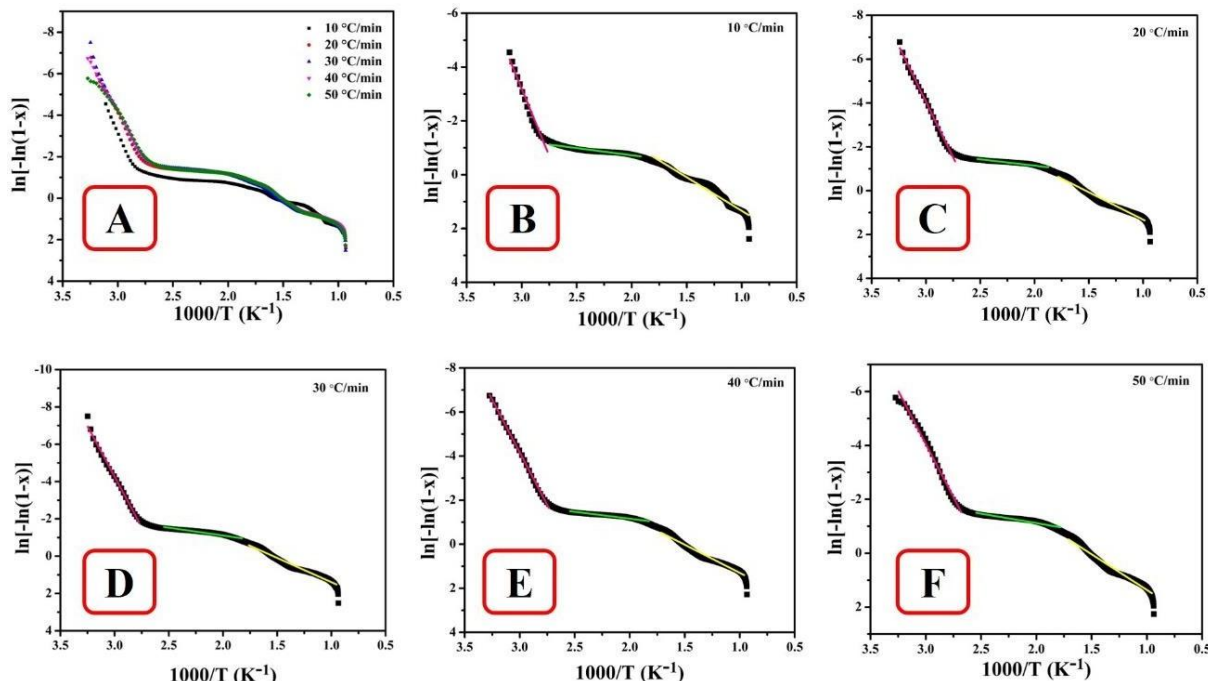


Figure 9. Plot of $\ln[-\ln(1-x)]$ vs $1000/T$ at different heating rate CG-CuNPs A) Overall heating rate (10 – 50 $^{\circ}\text{C}$), B) CG-CuNPs 10 $^{\circ}\text{C}/\text{min}$, C CG-CuNPs 20 $^{\circ}\text{C}/\text{min}$, D) CG-CuNPs 30 $^{\circ}\text{C}/\text{min}$, E) CG-CuNPs 40 $^{\circ}\text{C}/\text{min}$, F) CG-CuNPs 50 $^{\circ}\text{C}/\text{min}$

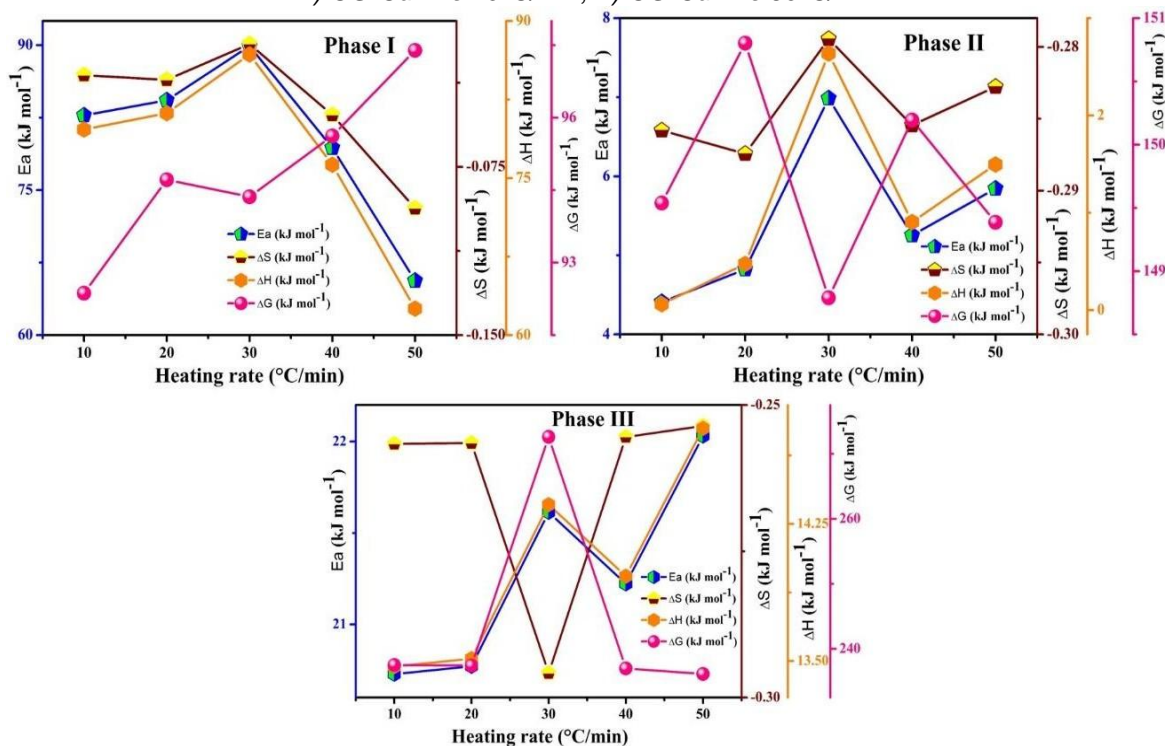


Figure 10. Thermal parameter of different heating rate at 100 $^{\circ}\text{C}$ (Stage I), 250 $^{\circ}\text{C}$ (Phase II) and 600 $^{\circ}\text{C}$ (Phase III)

Table 4. Thermodynamic parameters of SV-CuNPs at different heating rate at temperature (100, 250 and 600°C)

S. No	Heating rate (°C/min)	phase	Temp.(°C)	Ea (kJ mol ⁻¹)	ΔS (kJ mol ⁻¹)	ΔH (kJ mol ⁻¹)	ΔG (kJ mol ⁻¹)
1	10	1	100	82.7423	-0.0341	79.6410	92.3674
		2	250	4.4091	-0.2858	0.0607	149.5385
		3	600	20.7284	-0.2566	13.4700	237.5184
2	20	1	100	84.3004	-0.0362	81.1991	94.7145
		2	250	4.8223	-0.2874	0.4739	150.8026
		3	600	20.7716	-0.2565	13.5132	237.4273
3	30	1	100	89.9158	-0.0202	86.8146	94.3621
		2	250	6.9857	-0.2794	2.6373	148.7891
		3	600	21.6139	-0.2958	14.3555	272.6096
4	40	1	100	79.3758	-0.0519	76.2746	95.6220
		2	250	5.2538	-0.2854	0.9054	150.1938
		3	600	21.2223	-0.2555	13.9639	236.9874
5	50	1	100	65.6298	-0.0935	62.5285	97.3927
		2	250	5.8441	-0.2828	1.4957	149.3860
		3	600	22.0312	-0.2536	14.7728	236.1309

4. CONCLUSION

The generated unique nano material's -OH, C=O, C-H, C≡N, and CuNPs interaction are explained by the FT-IR spectra of SV-CuNPs and CG-CuNPs and their corresponding plant extracts. SV-CuNPs and CG-CuNPs' thermal stability was investigated using the TGA technique. Using a thermal analysis equipment, the thermal degradation behavior of the SV-CuNPs and CG-CuNPs was investigated at various heating speeds (10-50°C/min) in a nitrogen atmosphere. The thermal degradation kinetic parameters were determined using the Coats-Redfern non-isothermal kinetic model.

The TGA data demonstrated that SV-CuNPs and CG-CuNPs underwent three different stages of thermal degradation. It was agreed that the initial stage of moisture removal would be the heat degradation phase up to 100°C. The second stage of heat degradation, which relates to hemicellulose breakdown, happened up to 250°C. The final stage involved extracting CuNPs from the produced NPs. The changes in enthalpy (ΔH), entropy (ΔS), and Gibbs free energy (ΔG) that are indicative of thermodynamic characteristics reveal that SV-CuNPs and CG-NPs require external energy to commence pyrolysis kinetics. The positive ΔH values suggest this. Every model has a positive ΔG value, indicating that the SV-CuNPs and CG-NPs do not break down spontaneously. It suggests that both of the newly created copper nanoparticles are extremely thermally stable and can only be shattered with the addition of external energy.

At a heating rate of 30°C/min and 10°C/min, the highest and minimum Ea values of SV-CuNPs

from Phase I and II are 67.3290 kJ mol⁻¹ and 7.1086 kJ mol⁻¹ respectively. For CG-CuNPs in Phase I and II, the highest and minimum Ea values are found to be 89.9158 kJ mol⁻¹ and 4.4091 kJ mol⁻¹ respectively, at heating rates of 30°C/min and 10°C/min. This outcome unequivocally shows that CG-CuNPs are thermally more stable than SV-CuNPs.

5. REFERENCES

- [1] S.Z.A. Khader, S. Syed Zameer Ahmed, J. Sathyan, M.R. Mahboob, K. P. Venkatesh, K. Ramesh (2018) A comparative study on larvicidal potential of selected medicinal plants over green synthesized silver nano particles, Egypt. J. Basic Appl. Sci. 5, 54–62. doi:10.1016/j.ejbas.2018.01.002.
- [2] S. Yedurkar, C. Maurya, P. Mahanwar (2016) Biosynthesis of Zinc Oxide Nanoparticles Using *Ixora Coccinea* Leaf Extract—A Green Approach, Open J. Synth. Theory Appl. 05, 1–14. doi:10.4236/ojsta.2016.51001.
- [3] T.B. Devi, M. Ahmaruzzaman (2017) AgNPs-AC Composite for Effective Removal (Degradation) of Naphthol Green B Dye from Aqueous Solution, Chemistry Select. 2 9201–9210. doi:10.1002/slct.201700641.
- [4] R.T. V. Vimala, G. Rajivgandhi, S. Sridharan, M. Jayapriya, G. Ramachandran, C.C. Kanisha, N. Manoharan, W.-J. Li (2019) Biosynthesis and Characterization of Gold Nanoparticles from *Actinobacteria*, Int. J. Pharm. Sci. Res. 10, 4391–4395. doi:10.1007/978-1-0716-1728-1_104.
- [5] S. Dhiva, R. Bindu, V.K. Vijay (2021) A study on medicinal properties of *Coccinia grandis*, J. Trans. Environ. Technovation. 15, 8–12. doi:10.56343/stet.116.015.001.002.

- [6] T.B. Devi, D. Mohanta, M. Ahmaruzzaman (2019) Biomass derived activated carbon loaded silver nanoparticles: An effective nanocomposites for enhanced solar photocatalysis and antimicrobial activities, *J. Ind. Eng. Chem.* 76, 160–172. doi:10.1016/j.jiec.2019.03.032.
- [7] T.B. Devi, M. Ahmaruzzaman (2018) Facile preparation of Copper nanoparticles using *Coccinia grandis* fruit extract and its application towards the reduction of toxic nitrocompound, *Mater. Today Proc.* 5, 2098–2104. doi:10.1016/j.matpr.2017.09.206.
- [8] R. Khasawneh, R. Kornreich (2013) Antiurolihiatic Activity of the plant extracts of *Solanum Virginianum* on ethylene glycol induced urolithiasis in rats, *Int. J. Pharm.Biol. Sci.* 3, 328-334.
- [9] K. Saraswathi, R. Bharkavi, A. Khusro, C. Sivaraj, P. Arumugam, S. Alghamdi, A.S. Dabool, M. Almeahadi, A.M. Bannunah, M. Umar Khayam Sahibzada (2021) Assessment on in vitro medicinal properties and chemical composition analysis of *Solanum virginianum* dried fruits, *Arab. J. Chem.* 14, 103442. doi:10.1016/j.arabjc.2021.103442.
- [10] M.A. Farrukh, K.M. Butt, K.K. Chong, W.S. Chang (2019) Photoluminescence emission behavior on the reduced band gap of Fe doping in $\text{CeO}_2\text{-SiO}_2$ nanocomposite and photo physical properties, *J. Saudi Chem. Soc.* 23, 561–575. doi:10.1016/j.jscs.2018.10.002.
- [11] R. Arunachalam, S. Dhanasingh, B. Kalimuthu, M. Uthirappan (2012) Phytosynthesis of silver nanoparticles using *Coccinia grandis* leaf extract and its application in the photocatalytic degradation, *Colloid Surfaces B Biointerfaces.* 94, 226–230. doi:10.1016/j.colsurfb.2012.01.040.
- [12] K. Zapata, Y. Rodríguez, S.H. Lopera, F.B. Cortes, C.A. Franco (2022) Development of Bio-Nanofluids Based on the Effect of Nanoparticles' Chemical Nature and Novel *Solanum torvum* Extract for Chemical Enhanced Oil Recovery (CEOR) Processes, *Nanomaterials*, 12. doi:10.3390/nano12183214
- [13] S.G. Jebadurai, R.E. Raj, V.S. Sreenivasan, J.S. Binoj (2019) Comprehensive characterization of natural cellulosic fiber from *Coccinia grandis* stem, Elsevier Ltd., doi:10.1016/j.carbpol.2018.12.027

IZVOD

SINTEZA I KARAKTERIZACIJA NANOČESTICE BAKRA *SOLANUM VIRGINIANUM* IEKSTRAKT *COCCINIA GRANDIS*: KOMPARATIVNA STUDIJA O TERMIČKOM PONAŠANJU

Biogena, zelena metoda sinteze je opisana za nove nanočestice bakra iz ekstrakta listova Solanum Virginianum i Coccinia Grandis. Infracrvena spektroskopija sa Furije-transformacijom i termalna gravimetrijska analiza su korišćeni za ispitivanje rezultujućih nanočestica. Analiza sastava i proučavanje procesa kao što su isparavanje i raspadanje obavljene su termogravimetrijskom analizom. Isparljiva jedinjenja, koja je uzorak oslobodio, analizirana su korišćenjem TGA u kombinaciji sa infracrvenom spektroskopijom Furijeove transformacije (FTIR). Iz dobijenih FTIR podataka pokazalo se da i CG-CuNP i SV-CuNP uključuju funkcionalnu molekularnu strukturu. Pored toga, rezultati TGA su pokazali da SV-CuNP i CG-CuNP pokazuju efikasno ponašanje termičke stabilnosti, dok biljni ekstrakti iz Coccinia grandis i Solanum virginianum igraju glavnu ulogu u stvaranju nanočestica i takođe poboljšavaju njihovu termičku stabilnost.

Ključne reči: *Coccinia grandis, Solanum virginianum, zelena sinteza, nanočestice bakra, termička analiza*

Naučni rad

Rad primljen: 29.10.2023.

Rad korigovan: 12.04.2024.

Rad prihvaćen: 12.05.2024.

Rad je dostupan na sajtu: www.idk.org.rs/casopis

Anbarasu Prema, <https://orcid.org/0009-0000-8689-9296>

Raghunathan Muthuselvi, <https://orcid.org/0000-0001-6595-8576>

Ramaswami Vashantha, <https://orcid.org/0009-0002-5201-6656>